

Effect of flow geometry parameters on transient heat transfer for turbulent flow in a circular tube with baffle inserts

Ahmet Tandiroglu *

Department of Mechanical Engineering Technology, Vocational High School of Erzincan, Atatürk University, 24109 Erzincan, Turkey

Received 22 February 2005; received in revised form 30 September 2005

Available online 9 March 2006

Abstract

The effect of the flow geometry parameters on transient forced convection heat transfer for turbulent flow in a circular tube with baffle inserts has been investigated. The characteristic parameters of the tubes are pitch to tube inlet diameter ratio $H/D = 1, 2$ and 3 , baffle orientation angle $\beta = 45^\circ, 90^\circ$ and 180° . Air, Prandtl number of which is 0.71 , was used as working fluid, while stainless steel was considered as pipe and baffle material. During the experiments, different geometrical parameters such as the baffle spacing H and the baffle orientation angle β were varied. Totally, nine types of baffle inserted tube were used. The general empirical equations of time averaged Nusselt number and time averaged pressure drop were derived as a function of Reynolds number corresponding to the baffle geometry parameters of pitch to diameter ratio H/D , baffle orientation angle β , ratio of smooth to baffled cross-section area S_o/S_a and ratio of tube length to baffle spacing L/H were derived for transient flow conditions. The proposed empirical correlations were considered to be applicable within the range of Reynolds number $3000 \leq Re \leq 20,000$ for the case of constant heat flux.
© 2006 Elsevier Ltd. All rights reserved.

Keywords: Effects of flow geometry parameters; Transient forced convection; Circular tube with baffle inserts; Heat transfer augmentation

1. Introduction

Enhancement of heat transfer performance especially in shell and tube heat exchangers is succeeded by means of baffle inserts. As it known, various baffle shapes and different orientations have been the subject of several investigations. Augmentation techniques usually employ baffles attached to the heated surface so as to provide an additional heat transfer surface area and to promote turbulence. The majority of the work cited in baffle research deals with baffles oriented either parallel with the flow passage or perpendicular to it. A general criterion for determining the optimum baffle spacing for all types of shell and tube heat exchangers was established by Saffar-Avval and Damangir [1]. Berner et al. [2] researched with airflow over baffles for Reynolds numbers ranging from 600 to

10,500. After a sufficient development distance, they achieved a stream-wise periodic flow. They found this development distance to be a function of both the Reynolds's number and the geometry of the baffle. Lopez et al. [3] performed numerical studies of laminar convective heat transfer behavior in a three-dimensional channel with baffles. Hwang and Liou [4] researched by studying perforated baffles in turbulent flow. Both of these studies utilized straight baffles for flow and heat transfer. Dutta [5,6], Dutta and Dutta [7], Dutta et al. [8] investigated the effects of baffle size, perforation, and orientation on internal heat transfer enhancement. They found the dimension of the heat transfer surface and determined the optimum positioning of the baffles. Berner et al. [9] obtained experimental results of mean velocity and turbulence distributions in flow around segmented baffles. Experimental investigation of characteristics of the turbulent flow and heat transfer inside the periodic cell formed between segmented baffles staggered in a rectangular duct was studied by Habib et al. [10]. The experimental results indicated that the

* Tel.: +90 542 426 0973; fax: +90 446 226 6601.

E-mail address: atandir@atauni.edu.tr

Nomenclature

C_p	specific heat (kJ/kg K)
dP/dx	pressure gradient (N/m ³)
D	tube inlet diameter (m)
h	heat transfer coefficient (W/m ² K)
H	baffle spacing or pitch (m)
f	dimensionless pressure drop
k	thermal conductivity (W/m K)
L	tube length (m)
Pr	Prandtl number
Q	heat transferred to fluid
Re	Reynolds number
S	cross-sectional area
T	temperature (K)
t	time (s)
u	velocity (m/s)

Greek symbols

β	baffle orientation angle (°)
ρ	density (kg/m ³)
μ	dynamic viscosity (kg/m s)
ν	fluid kinematic viscosity (m ² /s)

Subscripts

a	baffle inserted tube
ave	average
b	bulk
o	smooth pipe
t	transient condition
w	wall

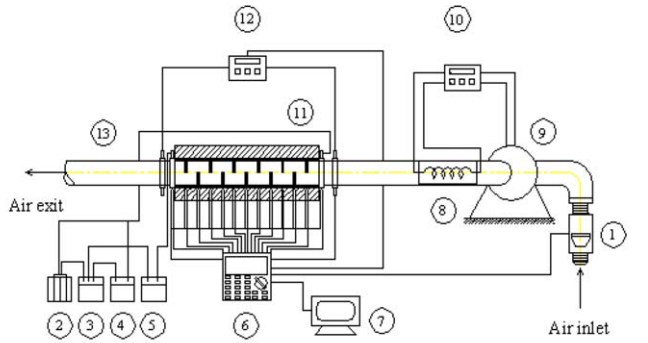
pressure loss increased as the baffle height did. For a given flow rate, local and average heat transfer parameters increase with increasing Reynolds number and baffle height. Numerical predictions of the flow and heat transfer in channels with staggered fins were investigated by Webb and Ramadhyani [11], Kelkar and Patankar [12], and Habib et al. [13]. A comparative performance study of seven different heat transfer enhancement technologies differed by geometry, flow conditions and operating temperatures and a reference smooth tube has been performed by Andrews and Fletcher [14]. In the performance comparisons a heat transfer rate was used as a function of pumping power parameter. The chosen performance parameters made sense but by necessity are dimensional, so a rescaling procedure was used to compare technologies. Recently, similar baffle geometries have been investigated experimentally and the empirical models of these kinds of flow geometries for steady state convective heat transfer were developed by Tandiroglu [15]. These empirical models were valid for a wide range of Reynolds number $3000 \leq Re \leq 20,000$. The present experimental correlations were compared with available correlation equations and experimental data. These comparisons show very good agreement for a turbulent flow convective heat transfer. Most recently, a comprehensive investigation of transient forced convective heat transfer for turbulent flow in a circular tube with baffle inserts has been presented by Tandiroglu [16]. Second law analysis has been performed as an enhancement technique to capture the best baffled tube having the least rate of entropy generation and augmentation entropy generation number. A generalized correlation for the unsteady entropy generation number relative to the steady dimensional entropy generation number for the same flow geometries has been developed in the form of $S_{gen,t} = S_{gen,\infty} + Be \frac{-Be}{e^{Be}}$. It is observed that baffle inserted tubes of the type 4562 exhibits the minimum rate of entropy generation number and minimum augmentation

entropy generation number for transient flow conditions as in the case of steady state flow condition.

As is seen, almost all of the studies in the above cited literature, there is no study which is conducted to analyze unsteady forced convective heat transfer in baffle inserted tubes which differ largely from each other due to their geometrical arrangements by means of first and second law analysis for turbulent flow except author's own investigation. The main objective of the present work is to derive empirical equations to correlate the time averaged friction factor, time averaged Nusselt number depending on baffle geometry parameters of pitch to diameter ratio H/D , baffle orientation angle β , ratio of smooth to baffled cross-section area S_o/S_a and ratio of tube length to baffle spacing L/H . The proposed correlations are considered to be applicable within the range of Reynolds number $3000 \leq Re \leq 20,000$ for the case of constant heat flux. To this end, present investigation has been undertaken and it is intended to contribute to the previous and further studies.

2. Experimental apparatus

A schematic diagram of experimental setup is illustrated in Fig. 1. Air was used as a working fluid. Experimental setup mainly consists of flow entrance section, flow development section, test section and flow exit section. Experimental setup is fabricated completely from stainless steel of type AISI 304L which is an austenitic stainless steel has a ground finish produced by grinding a tube with an abrasive belt impregnated with No. 180 grit and was insulated with 25-mm thick multilayer glass wool to inhibit heat losses. A total of nine samples of baffle inserted tubes having half circle geometry were investigated. Half circle baffles made of type AISI 304L were set in tube which has an inner diameter of 31 mm and the thickness of 2 mm. The flow geometries and parameters investigated in this study were explained as follows and are shown in



- 1 Air flow sensor
- 2 DC power supply
- 3 Watt meter
- 4 Volt meter
- 5 Amper meter
- 6 Data acquisition system
- 7 PC control unit
- 8 Constant temperature heater
- 9 Adjustable speed exhaust fan system
- 10 Fan speed and heater controller
- 11 Test section
- 12 Differential pressure sensor
- 13 Flow exit section

Fig. 1. Schematic diagram of the experimental setup.

Fig. 2. Periodically 45° opposite-oriented baffle inserted tube has several baffles with the pitch to diameter ratios H/D were from 1 to 3 and the orientation angle β was kept 45°, which is shown in Fig. 2a. Periodically 90° opposite-

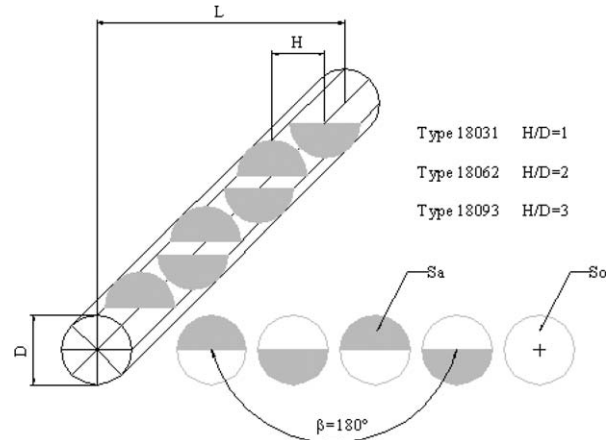


Fig. 2c. Schematic of 180° half circle baffled tubes.

oriented baffle inserted tube has several baffles with the pitch to diameter ratios H/D were from 1 to 3 and the orientation angle β is kept 90°, which is shown in Fig. 2b. Periodically 180° opposite-oriented baffle inserted tube has several baffles with the pitch to diameter ratios H/D were from 1 to 3 and the orientation angle β is kept 180°, which is shown in Fig. 2c. The detailed geometrical parameters of baffled tubes were tabulated in Table 1.

The heat loss calibration tests were performed before taking measurements on the system for each type of baffle inserted tubes in the following manner. Each baffle inserted tube was completely filled up with insulation materials of multilayer glass wool and constant heat flux was supplied through the pipe wall by means of PLC integrated DC power supply. The average wall temperatures were evaluated at 11 points along the test section in terms of heat flux, difference in wall and ambient temperatures. The time averaged wall temperature variations by time were recorded using data online acquisition system. When the steady state condition is established to insure that external thermal equilibrium can be achieved, heat loss calibration tests for different values of power supply are reported for a steady state case. It was found that the heat loss is directly proportional to the difference between the wall and ambient temperatures. The required constant of proportionality was taken from the previously determined heat

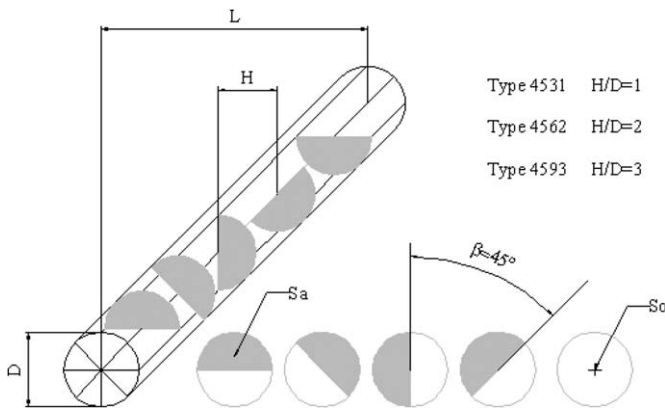


Fig. 2a. Schematic of 45° half circle baffled tubes.

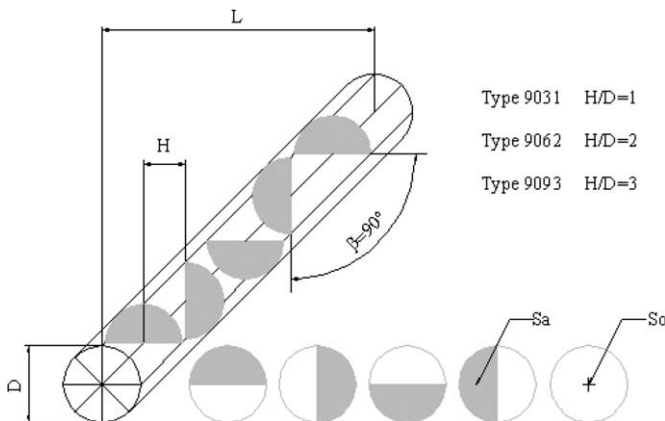


Fig. 2b. Schematic of 90° half circle baffled tubes.

Table 1
The characteristics of baffle inserted tubes

Baffle types	β (°)	H ($\times 10^{-3}$ m)	H/D
18031	180	31	1
18062	180	62	2
18093	180	93	3
9031	90	31	1
9062	90	62	2
9093	90	93	3
4531	45	31	1
4562	45	62	2
4593	45	93	3

loss calibrations. It was observed that the maximum heat loss did not exceed 5% all through the test runs. More detailed explanation of the heat loss calibration technique was given by Tandiroglu [15]. The steady state experiment results were compared with existing smooth tube correlations. Time averaged wall temperature variations with heat loss were calibrated for unsteady state flow cases by using the method mentioned above. Heat loss calibration test results were also checked by heat transferred to fluid obtained by mass flow rate and the temperature difference of the wall and ambient temperature.

The experiments were conducted mainly in the test section for all flow geometries. The effect of thermal radiation for internal flow is ignored during the experiments due to low temperature difference between wall and baffle. Eleven pipe clamp temperature sensors of type CrNi–Cr were installed along the length of 1 m baffle inserted test tubes to measure its surface temperatures. Rotating vane air flow meter is used in order to measure air flow rates passing through the system. An adjustable temperature controlled air heater was installed into flow entrance section to introduce constant temperature air through the system. The mean air temperatures entering and leaving the test section are measured by CrNi–Cr immersion type temperature measuring sensors. All used temperature sensors of type CrNi–Cr have $\pm 0.05\%$ full scale accuracy and no sensor calibration settings required because of common features of all ALMEMO sensors.

Experimental setup was equipped with data online acquisition system including display and operating control of type ALMEMO 5590-2 which is entirely new generation of measuring system to monitor and record measuring points for all of the test runs continuously. The intelligent ALMEMO connectors are patented and have been especially designed for directly connecting more than 65 types of sensors such as temperature, rotating vane air flow meter, differential pressure and peripheral equipment. They include EEPROM where sensor and device parameters are stored. Connected sensors are automatically detected and the functions are adapted correspondingly, giving the data online acquisition system is unsurpassed flexibility and ease of operation. When connecting intelligent sensor connectors to the data online acquisition system the measuring range, accuracy, gain, required power supply and reference junction compensation are automatically transmitted to the data online acquisition system. Accurate measuring data can be read immediately without instrument calibration settings required. The relevant measuring channels are automatically activated and properly set by the sensors with intelligent ALMEMO pre-programmed connectors. Faulty measurements caused by wrong manual programming or confusion of sensors are totally impossible.

During the experiments, the adjustable speed exhaust fan system was turned on and constant temperature fresh air was drawn through the inlet section into the test section. The flow rate was set in such a way that the pressure drop across the upstream and downstream of the test section

corresponds to the required Reynolds number. After the flow was set across the test section, constant heat flux was induced to test section directly by means of PLC integrated DC power supply which could be regulated in the ranges of 0–60 V and 0–660 A. Data for all the measuring points were recorded and finally averaged over the elapsed time simultaneously by means of data online acquisition system till the system was allowed to approach the steady state. At steady state the temperatures of the pipe clamp temperature sensors were noted by data acquisition system and logged by the computer. All these measurements along with the test runs were collected, processed, stored, analyzed and displayed by a PC through the data acquisition system. The whole process was controlled with a computer program developed specially for this experimental study.

3. Data reduction

The goal of this experimental study is to determine Nusselt numbers of the baffle inserted tubes for fully developed turbulent flow. The independent parameters are Reynolds number and tube diameter. The Reynolds numbers based on the tube hydraulic diameter are given by

$$Re = \frac{uD}{\nu} \quad (1)$$

The average fully developed heat transfer coefficients are evaluated from the measured temperatures and heat inputs

$$h = \frac{Q}{(T_w - T_b)A}, \quad (2)$$

where A is convective heat transfer area. Then full developed Nusselt numbers are evaluated by using

$$Nu = \frac{hD}{k} \quad (3)$$

It may be noted that for periodically fully developed flow, the pressure exhibits periodicity character similar to those already ascribed to the temperature. The pressure at successive points lies on straight line as well as temperatures of the same set of points. With this, the friction factor is evaluated using

$$f = \frac{-\frac{dp}{dx} D}{\frac{1}{2} \rho u^2}, \quad (4)$$

where $\frac{dp}{dx}$ is pressure gradient.

To describe the effects of the flow conditions and geometry parameters of Reynolds number Re , Prandtl number Pr , pitch to diameter ratio H/D , baffle orientation angle β , ratio of smooth to baffled cross-section area S_o/S_a and ratio of tube length to baffle spacing L/H on transient forced convection heat transfer for turbulent flow in a circular tube with baffle inserts, time averaged Nusselt number is related as:

$$Nu_{ave(t)} = f_1(Re, Pr, (H/D), (S_o/S_a), \beta, (L/H)). \quad (5)$$

In Eq. (5), the Prandtl number Pr , which should be an important parameter affecting the heat transfer of baffle inserted tube, is defined as

$$Pr = \frac{C_p \mu}{k}. \quad (6)$$

But, Prandtl number has not been separately considered in this investigation because air is only used as working fluid and its Prandtl number in the considered experimental range temperature range remains almost constant. So, Eq. (6) can be simplified as:

$$Nu_{ave(t)} = f_1(Re, (H/D), (S_o/S_a), \beta, (L/H)). \quad (7)$$

Similarly, a relationship for the friction factor f of a turbulent flow through a transient forced convection heat transfer for turbulent flow in a circular tube with baffle inserts can then be proposed for its generalization in terms of Reynolds number Re , pitch to diameter ratio H/D , baffle orientation angle β , ratio of smooth to baffled cross-section area S_o/S_a and ratio of tube length to baffle spacing L/H on transient forced convection heat transfer for turbulent flow in a circular tube with baffle inserts as shown below for the time averaged friction factor:

$$f_{ave(t)} = f_2(Re, (H/D), (S_o/S_a), \beta, (L/H)). \quad (8)$$

4. Experimental uncertainty analysis

The uncertainties of experimental quantities were computed by using the method presented by Kline and McClintock [17]. The uncertainty calculation method used involves calculating derivatives of the desired variable with respect to individual experimental quantities and applying known uncertainties. The general equation presented by Kline and McClintock [17] showing the magnitude of the uncertainty in $R(uR)$ is

$$u_R = \pm \left[\left(\frac{\partial R}{\partial x_1} u_{x_1} \right)^2 + \left(\frac{\partial R}{\partial x_2} u_{x_2} \right)^2 + \cdots + \left(\frac{\partial R}{\partial x_n} u_{x_n} \right)^2 \right]^{1/2}, \quad (9)$$

where $R = R(x_1, x_2, \dots, x_n)$ and x_n is the variable that affects the results of R .

The experimental results up to a Reynolds number of 20,000 were correlated with a standard deviation of 5% at most. Experimental uncertainties in the Reynolds number, friction factor, and Nusselt number were estimated by the above procedure described in [17]. The mean uncertainties are $\pm 2.5\%$ in the Reynolds number, $\pm 4\%$ in the friction number. The highest uncertainties are $\pm 9\%$ in the Nusselt number for the type 9031. Uncertainties in the Nusselt number range between $\pm 5\%$ and 8% for $3000 \leq Re \leq 20,000$ at the type 18093 and $\pm 8\%$ and 10% $3000 \leq Re \leq 20,000$ at the type 9031, highest uncertainties being at the lowest Reynolds number.

5. Results and discussion

5.1. Confirmatory tests

The present experimental results on heat and fluid flow characteristics in a smooth tube were firstly reported in the form of Nusselt number and friction factor. The results of the smooth tube were compared with the results obtained from the well-known steady state flow correlations of Dittus and Boelter [18], Sieder and Tate [19], Petukhov [20], Moody [21] and Gnielinski [22] for the fully developed turbulent flow in circular tubes. Nusselt number correlations:

Correlation from Dittus and Boelter [18] is of the form:

$$Nu = 0.023 Re^{0.8} Pr^{0.4} \quad \text{for } Re \geq 10,000.$$

Correlation from Sieder and Tate [19] is of the form:

$$Nu = 0.027 Re^{0.8} Pr^{1/3} \left(\frac{\mu_b}{\mu_w} \right)^{0.14} \quad \text{for } Re \geq 10,000.$$

Correlation from Petukhov [20] is of the form:

$$Nu = \frac{(f/8) Re Pr}{1.07 + 12.7(f/8)^{1/2} (Pr^{2/3} - 1)}$$

for $10^4 \leq Re \leq 5 \times 10^6$.

Correlation from Gnielinski [22] is of the form:

$$Nu = \frac{(f/8) Re Pr}{1 + 12.7(f/8)^{1/2} (Pr^{2/3} - 1)}$$

for $2300 \leq Re \leq 5 \times 10^6$.

Friction factor correlations: correlation from Moody diagram (see [21]) is of the form:

$$f = 0.316 Re^{-0.25} \quad \text{for } Re \leq 2 \times 10^4.$$

Correlation from Petukhov [20] is of the form:

$$f = (1.82 \ln Re - 1.64)^{-2} \quad \text{for } 10^4 \leq Re \leq 5 \times 10^6.$$

Correlation from Gnielinski [22] is of the form:

$$f = (0.79 \ln Re - 1.64)^{-2} \quad \text{for } 2300 \leq Re \leq 5 \times 10^6.$$

Figs. 3 and 4 show comparison between the present experimental work and the past correlations from previous works available for steady state flow conditions in the literature for smooth tube. As it can be shown in Figs. 3 and 4, the present work agrees well with the available correlations with $\pm 13\%$ and 11% in comparison with Petukhov correlation and Gnielinski correlation, respectively, for the friction factor, and $\pm 18\%$ in comparison with Dittus–Boelter, Sieder and Tate for the Nusselt number.

5.2. Heat transfer

In the present article, experimental measurements of both heat transfer and pressure drop in a tube with baffle inserts for a transient heat transfer are presented. The

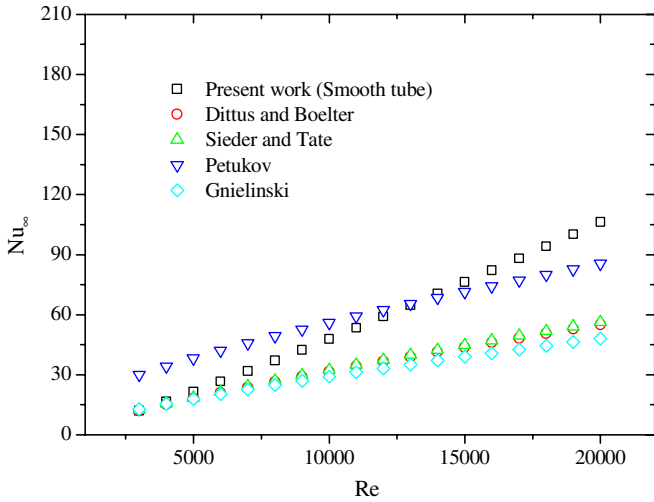


Fig. 3. Data verification of Nusselt number for smooth tube.

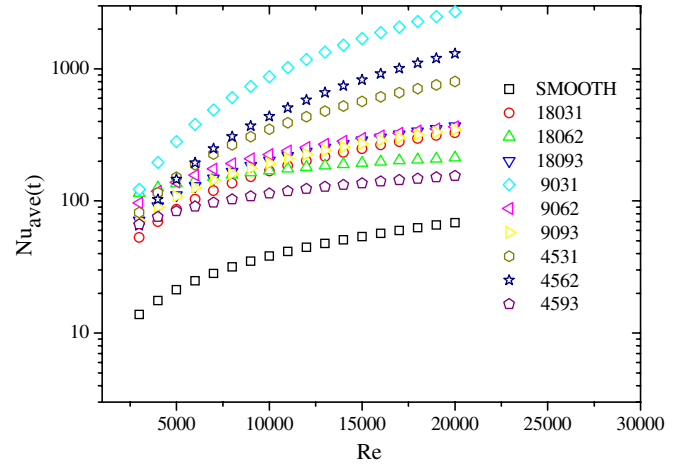


Fig. 5a. The time averaged Nusselt number with respect to Reynolds number.

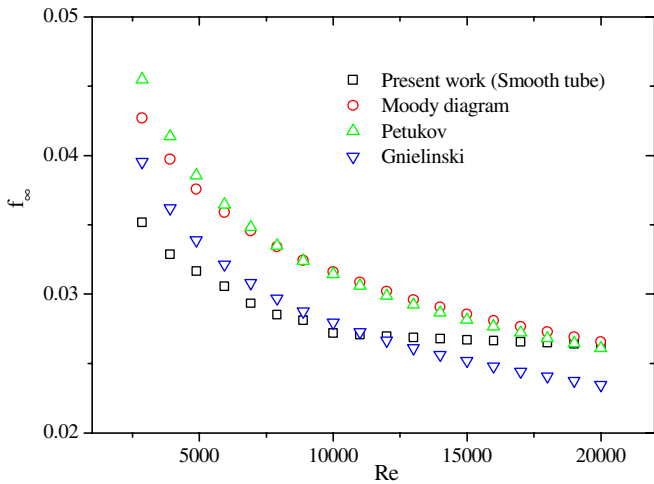


Fig. 4. Data verification of friction factor for smooth tube.

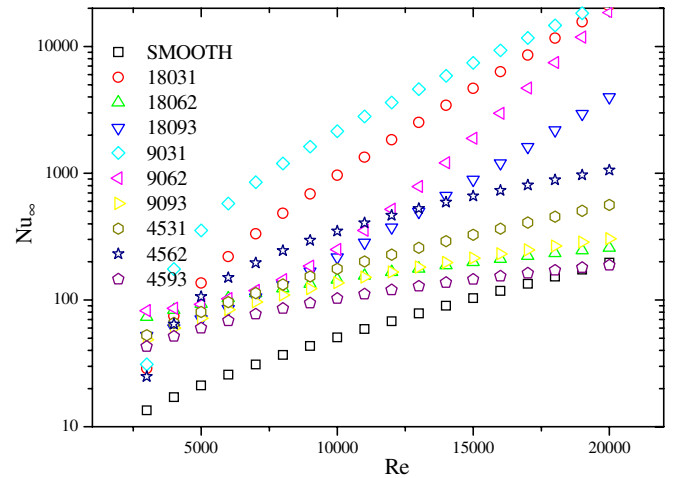


Fig. 5b. Nusselt number versus Reynolds number for steady state flow condition.

pressure drops corresponding to the heat transfer enhancement due to the baffle plate arrangements in the tube were measured under heated flow conditions. The time averaged Nusselt number and steady state condition of Nusselt number are plotted in Figs. 5a and 5b, respectively, as a function of Reynolds number, for all kinds of flow geometries. The effect of baffle inserted in a circular tube on transient heat transfer is shown in Fig. 5a. As shown, the time averaged Nusselt number increases with increasing Reynolds number. It is found that the tubes with baffle inserts give higher heat transfer rate than the smooth tube. It is clear from Fig. 5a that the highest time averaged Nusselt Number was achieved with baffle inserted tube of the type 9031. In this type of 9031 increase in the time averaged Nusselt number was obtained at least 786% as compared to the smooth tube. Fig. 5b shows the changes of Nusselt number with Reynolds number for all types of baffle inserted tubes. It was observed from this figure that the

Nusselt number increased with the increase of Reynolds number. The highest Nusselt number was obtained in the type of 9031 as in the case of transient flow conditions as shown in Fig. 5a. The increase in steady state Nusselt number was obtained at least 130% as compared to the type of 9031 with smooth tube. It is possible to observe that the time averaged Nusselt number value is higher when compared with the steady state flow case of Nusselt number.

5.3. Pressure drop

The measurements were converted to time averaged friction factor f using Eq. (4). The time averaged friction factor f variations with respect to Reynolds number is plotted in Figs. 6a and 6b as a function of Reynolds number for transient and steady state flow conditions, respectively. In spite

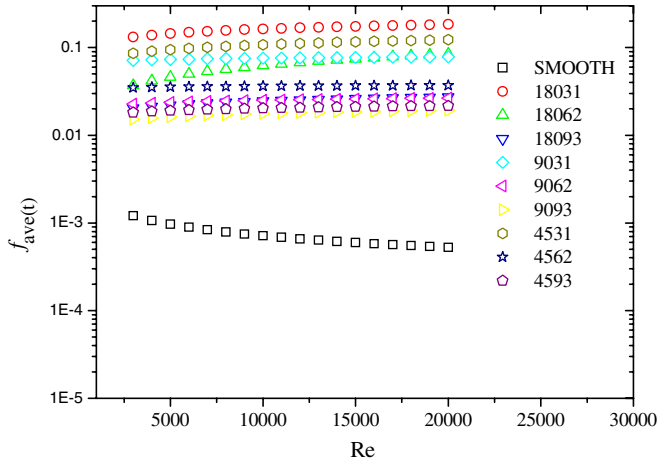


Fig. 6a. The time averaged friction factor f with respect to Reynolds number.

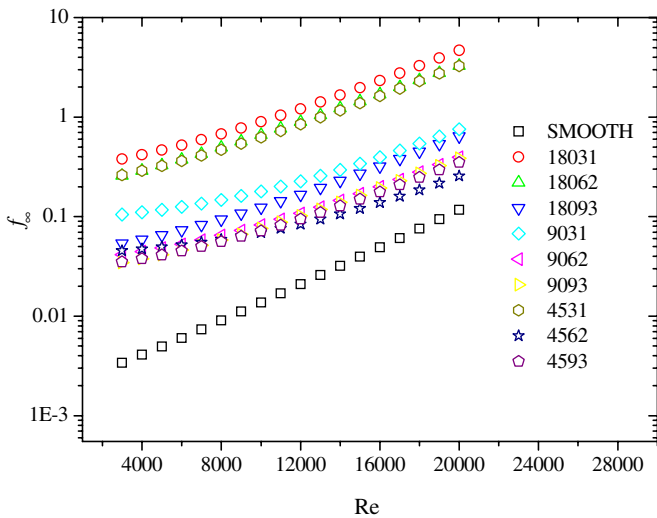


Fig. 6b. Friction factor f with respect to Reynolds number for steady state flow.

of the fact that pressure drops increase with increasing Reynolds numbers for both transient and steady state flow conditions, the rate of pressure drop increases with increasing Reynolds number for transient flow conditions, but decreases with increasing Reynolds numbers for the steady state flow conditions. The rate of average pressure drop in the baffle inserted tubes for transient flow conditions is higher than that of steady state flow conditions as well.

5.4. Empirical correlations

The heat transfer and pressure drop coefficients are commonly calculated from empirical correlations based on non-dimensional analysis and experimental data. Time averaged Nusselt number and time averaged pressure drop empirical correlations are obtained by correlating mea-

sured heat transfer and pressure drop coefficients by means of appropriate dimensionless numbers. For forced convection correlations are commonly expressed as a function of the Nusselt Nu , Prandtl Pr , Reynolds Re numbers and flow geometry parameters with a functional form. It is shown in this present work that time averaged Nusselt number and time averaged pressure drop depend on the Reynolds number, Prandtl number, pitch to diameter ratio, baffle orientation angle, ratio of smooth to baffled cross-section area and ratio of tube length to baffle spacing on transient forced convection heat transfer for turbulent flow in a circular tube with baffle inserts. The general empirical correlation was derived to correlate the time averaged Nusselt number with the independent parameters mentioned above in the form of:

$$Nu_{ave(t)} = 14.84Re^{1.34} Pr^{0.4} (H/D)^{-8.15} (S_o/S_a)^{-21.14} \beta^{-0.34} (L/H)^{-6.9}. \quad (10)$$

In the same manner, utilizing the experimental database for the general time averaged pressure drop can also be expressed as a function of Reynolds number, Prandtl number and flow geometry parameters for transient forced convection heat transfer in the form of:

$$f_{ave(t)} = 12.54Re^{0.16} Pr^{0.4} (H/D)^{-7.35} (S_o/S_a)^{-18.99} \beta^{0.37} (L/H)^{-5.7}. \quad (11)$$

The coefficient a and the exponents b, k, p, n, m depending on the flow geometry parameters are determined and tabulated in Tables 2 and 3 to obtain time averaged Nusselt number and time averaged pressure drop correlations for individual baffle inserted tube types based on the experimental, respectively.

Empirical correlations given in Eqs. (10) and (11) are valid for the Reynolds number ranged from 3000 to 20,000. Error estimations have been carried out the maximum percentage deviations between the experimental and predicted values are found to be $\pm 1\%$ for $Nu_{ave(t)}$ and $f_{ave(t)}$ for each type of baffle data.

The experimentally observed data were compared against the empirically predicted correlations in Figs. 7a and 7b for time averaged pressure drop and time averaged Nusselt number, respectively. The empirical correlation of time averaged pressure drop predicted 99% of the each set of data within $\pm 99\%$ accuracy, while it was 87% for general correlation. The time averaged Nusselt number data were predicted by empirical correlation in a similar manner, with 99% of the each set of data within $\pm 99\%$ accuracy. However, this accuracy was 68% for the general correlation. The equations of the simplest curve which statistically best fits the data for time averaged pressure drop and time averaged Nusselt number are illustrated as straight lines in Figs. 7a and 7b, respectively. These straight lines pass within the uncertainty range of each data point, that is, within the error bars. It may be noticed that the general correlations predict the time averaged pressure

Table 2
Correlation constants of empirically developed time averaged Nusselt number for baffle inserted tubes

Baffle types	<i>a</i>	<i>b</i>	<i>k</i>	<i>p</i>	<i>n</i>	<i>m</i>
$Nu_{ave(t)} = aRe^b Pr^{0.4} (H/D)^k (S_o/S_a)^p \beta^n (L/H)^m$						
General	14.83638	1.366326	-8.15350	-21.1406	-0.337777	-6.88380
18031	0.9408460	0.9632640	0.1000000	45.2795200	60.5274300	-30.6604000
18062	0.7486430	0.3242990	14.1321000	14.1321000	16.7614800	-13.4195000
18093	0.7396940	0.8663830	102.5934000	99.6613400	100.3684000	-129.733000
9031	0.7278720	1.6318580	0.1000000	-66.8957000	-47.7943000	17.6078500
9062	1.3401000	0.7001770	107.9605000	107.9605000	80.2213600	-69.5684000
9093	0.2714550	0.8380700	84.8167800	78.8516800	61.1780900	-76.0625000
4531	0.2393070	1.2053650	0.1000000	62.4050300	-29.4807000	-15.8123000
4562	1.4994510	1.5793570	121.4378000	121.4377000	-58.0533000	-55.8977000
4593	1.1689710	0.4444040	24.2031500	22.4629800	-13.4727000	-19.5124000

Table 3
Correlation constants of empirically developed time averaged pressure drop for baffle inserted tubes

Baffle types	<i>a</i>	<i>b</i>	<i>k</i>	<i>p</i>	<i>n</i>	<i>m</i>
$f_{ave(t)} = aRe^b Pr^{0.4} (H/D)^k (S_o/S_a)^p \beta^n (L/H)^m$						
General	12.54022	0.163636	-7.34577	-18.9913	0.374615	-5.69689
18031	0.0570560	0.1730260	0.1000000	0.0531200	0.0222190	-0.1368330
18062	0.0125770	0.4345670	-0.1008300	-0.1008300	-0.2320660	-0.6870140
18093	0.0045990	0.1531940	0.0841110	0.0899800	0.0834510	0.6663700
9031	0.0188060	0.0481970	0.1000000	0.1368410	0.1240510	0.2750680
9062	0.0052420	0.0823430	0.1411280	0.1411280	0.1267710	0.2592110
9093	0.0039020	0.1230550	0.1089330	0.1056370	0.1036680	0.1188590
4531	0.0399410	0.1860960	0.1000000	0.0466020	0.1184760	-0.1705110
4562	0.0092760	0.0315580	0.1730960	0.1730960	0.0742450	0.3743650
4593	0.0048170	0.0920320	0.1547100	0.1345170	0.0879460	0.2143220

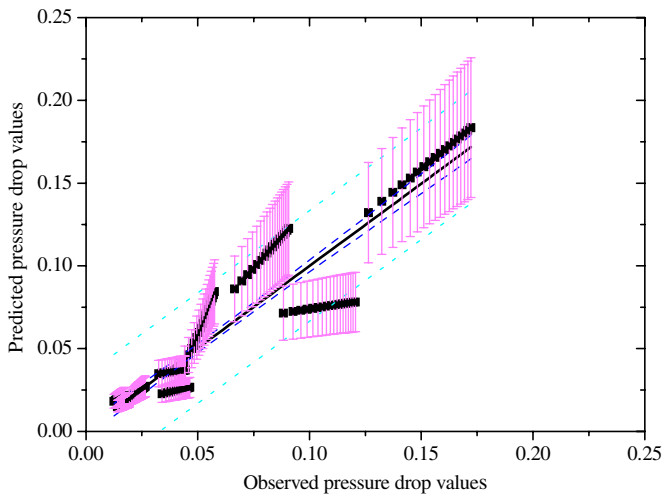


Fig. 7a. Comparison of correlation performance against baffle inserts pressure drop data.

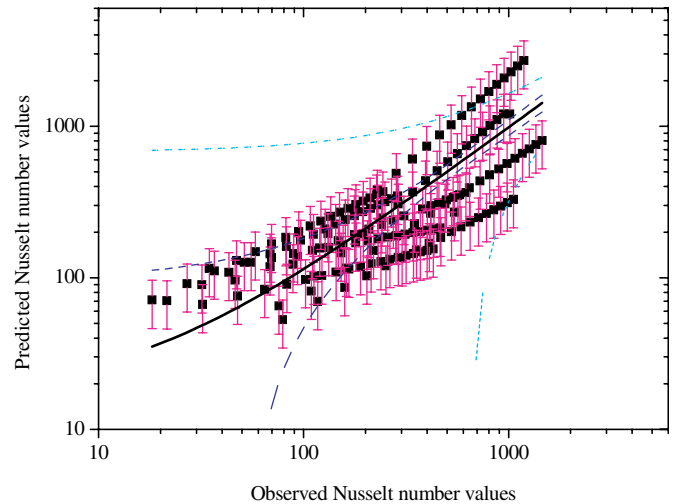


Fig. 7b. Comparison of correlation performance against baffle inserts Nusselt number data.

drop data better than the Nusselt number data. The reason for slightly less prediction performance of general empirical correlations is due mainly to the variety of the flow geometries which contained provisions to take into account the various effects caused by the pitch to diameter ratio, baffle orientation angle, ratio of smooth to baffled cross-section area, ratio of tube length to baffle spacing, and the Reynolds number and the Prandtl number.

6. Conclusions

The present study has focused on the investigation of forced convection and flow friction characteristics of a transient turbulent flow in a circular pipe with baffle inserts. A comprehensive experimental study has been carried out on nine baffle inserted tubes within the range of

Reynolds number $3000 \leq Re \leq 20,000$ for the case of constant heat flux. General empirical relations, which will be useful for estimation of flow geometry optimizations, have been proposed for time averaged Nusselt number and time averaged pressure drop as functions of Reynolds numbers and flow geometry parameters.

The empirical correlation of time averaged pressure drop predicted 99% of the each set of data within $\pm 99\%$ accuracy, while it was 87% for the general correlation have the form of

$$f_{ave(t)} = 12.54 Re^{0.16} Pr^{0.4} (H/D)^{-7.35} (S_o/S_a)^{-18.99} \beta^{0.37} (L/H)^{-5.7}.$$

The time averaged Nusselt number data were predicted by empirical correlation in a similar manner, with 99% of the each set of data within $\pm 99\%$ accuracy. However, this number was 68% for the general correlation have the form of

$$Nu_{ave(t)} = 14.84 Re^{1.34} Pr^{0.4} (H/D)^{-8.15} (S_o/S_a)^{-21.14} \beta^{-0.34} (L/H)^{-6.9}.$$

It may be noticed that the general correlations predict the time averaged pressure drop data better than the Nusselt number data. Experimental uncertainties in the Reynolds number, friction factor, and Nusselt number were estimated by the procedure described in [17]. The mean uncertainties are ± 2.5 in the Reynolds number, ± 4 in the friction factor. The maximum percentage deviations for the experimental and proposed correlation values of $Nu_{ave(t)}$ and $f_{ave(t)}$ were found to be $\pm 1\%$ for each type of baffle data curve. It can therefore be concluded that the proposed correlations are reasonably satisfactory for the prediction of time averaged Nusselt number and time averaged pressure drop for baffle inserted tubes.

Acknowledgements

The author gratefully acknowledges Professor Teoman Ayhan of the University of Bahrain for valuable suggestions and stimulating discussions about this work. Discussions with Professor Ibrahim Dincer of the University of Ontario Institute of Technology (UOIT) and Professor Mazhar Unsal of Fatih University are also appreciated. The author expresses his cordial thanks to the referees for valuable suggestions and comments to improve the presentation of this article.

References

- [1] M. Saffar-Avval, E. Damangir, A general correlation for determining optimum baffle spacing for all types of shell and tube exchangers, *Int. J. Heat Mass Transfer* 38 (1995) 2501–2506.
- [2] C. Berner, F. Durst, D.M. McEligot, Flow around baffles, *ASME J. Heat Transfer* 106 (1984) 743–749.
- [3] J.R. Lopez, N.K. Anand, L.S. Flecher, A numerical analysis of laminar convective heat transfer in a three-dimensional channel with baffles, in: *Proceedings of the Third U.S. National Congress on Computational Mechanics*, Dallas, TX, vol. 1, 1995, pp. 406–416.
- [4] J.J. Hwang, T.M. Liou, Heat transfer and friction in a low-aspect-ratio rectangular channel with staggered perforated ribs on two opposite walls, *ASME J. Heat Transfer* 117 (1995) 843–850.
- [5] P. Dutta, Cooling opportunity in advanced turbine system (ats) row one vane, a report on industrial projects submitted to the advanced gas turbine systems research, Clemson, SC, 1997.
- [6] P. Dutta, Innovative heat transfer enhancement with inclined solid and perforated baffles, MS Thesis, University of South Carolina, Columbia, SC, 1997.
- [7] P. Dutta, S. Dutta, Effect of baffle size, perforation, and orientation on internal heat transfer enhancement, *Int. J. Heat Mass Transfer* 41 (1998) 3005–3013.
- [8] S. Dutta, P. Dutta, R.E. Jones, J.A. Khan, Heat transfer coefficient enhancement with perforated baffles, *ASME J. Heat Transfer* 120 (1998) 795–797.
- [9] C. Berner, F. Durst, D.M. McEligot, Streamwise-periodic flow around baffles, in: *Proceedings of the 2nd International Conference on Applications of Laser Anemometry to Fluid Mechanics*, Lisbon, Portugal, 1984.
- [10] M.A. Habib, A.M. Mobarak, M.A. Sallak, E.A. Abdel Hadi, R.I. Affify, Experimental investigation of heat transfer and flow over baffles of different heights, *Trans. ASME J. Heat Transfer* 116 (1994) 363–368.
- [11] B.W. Webb, S. Ramadhyani, Conjugate heat transfer in a channel with staggered ribs, *Int. J. Heat Mass Transfer* 28 (1985) 1679–1687.
- [12] K.M. Kelkar, S.V. Patankar, Numerical prediction of flow and heat transfer in parallel plate channel with staggered fins, *Trans. ASME J. Heat Transfer* 109 (1987) 25–30.
- [13] M.A. Habib, A.E. Attya, D.M. McEligot, Calculation of turbulent flow and heat transfer in channels with streamwise-periodic flow, *Trans. ASME J. Turbomach.* 110 (1988) 405–411.
- [14] M.J. Andrews, L.S. Fletcher, Comparison of heat transfer technologies for gas heat exchangers, *ASME J. Heat Transfer* 118 (4) (1996) 897–902.
- [15] A. Tandiroglu, Akıŝa dik ynde engel bulunduran borularda akıŝım ve ısı transferinin incelenmesi, Ph.D. Thesis, Department of Mechanical Engineering, Karadeniz Technical University, Turkey, 2000 (in Turkish).
- [16] A. Tandiroglu, Second law analysis of transient heat transfer for turbulent flow in a circular tube with baffle inserts, *Int. J. Exergy* (IJEX) 2 (3) (2005) 299–317.
- [17] S.J. Kline, F.A. McClintock, Describing uncertainties in single sample experiments, *Mech. Eng.* 75 (1953) 385–387.
- [18] F.W. Dittus, L.M.K. Boelter, University of California Publications on Engineering, 2 443, Berkley, 1930.
- [19] E.N. Sieder, G.E. Tate, Heat transfer and pressure drop in liquids in tubes, *Ind. Eng. Chem.* 28 (1936) 1429–1435.
- [20] B.S. Petukhov, Heat transfer in turbulent pipe flow with variable physical properties, in: T.F. Irvine, J.P. Hartnett (Eds.), *Advances in Heat Transfer*, vol. 6, Academic Press, New York, 1970, pp. 504–564.
- [21] L.F. Moody, Friction factors for pipe flow, *Trans. ASME* 66 (1944) 671–684.
- [22] V. Gnielinski, New equations for heat and mass transfer in turbulent pipe flow and channel flow, *Int. Chem. Eng.* 16 (1976) 359–368.